

1 **Combining auxin-induced degradation and RNAi screening identifies**
2 **novel genes involved in lipid bilayer stress sensing in**
3 ***Caenorhabditis elegans***

4 Richard Venz^{1§}, Anastasiia Korosteleva¹ and Collin Y. Ewald^{1*}

5

6 **1** Eidgenössische Technische Hochschule Zürich, Department of Health Sciences and
7 Technology, Institute of Translational Medicine, Schwerzenbach-Zürich CH-8603, Switzerland

8 *Corresponding author: collin-ewald@ethz.ch (CYE)

9

10 **Keywords:**

11 Lipid bilayer stress, Lipotoxicity, Unfolded Protein Stress, Auxin-induced degradation,
12 CREB3, NRF2, MDT-15

13

14 **Abstract**

15 Alteration of the lipid composition of biological membranes interferes with their function
16 and can cause tissue damage by triggering apoptosis. Upon lipid bilayer stress, the
17 endoplasmic reticulum mounts a stress response that is similar to the unfolded protein
18 response. However, only a few genes are known to regulate lipid bilayer stress. Here,
19 we performed a suppressor screen that combined the auxin-inducible degradation
20 (AID) system with conventional RNAi in *C. elegans* to identify members of the lipid
21 bilayer stress response. AID-mediated knockdown of the mediator MDT-15, a protein
22 required for the upregulation of fatty acid desaturases, caused activation of a lipid
23 bilayer stress sensitive reporters. We screened through almost all *C. elegans* kinases
24 and transcription factors using RNAi by feeding. We report the identification of 8 genes
25 that have not been implicated previously with lipid bilayer stress before in *C. elegans*.
26 These suppressor genes include *skn-1/NRF1,2,3* and *let-607/CREB3*. Our candidate
27 suppressor genes suggest a network of transcription factors and the integration of
28 multiple tissues for a centralized lipotoxicity response in the intestine. Additionally, we
29 propose and demonstrate the proof-of-concept for combining AID and RNAi as a new
30 screening strategy.

31

32 **Introduction**

33 Biological membranes play an important role in protein folding, signaling, secretion,
34 and turnover of proteins. Changes in the lipid composition of a membrane alters its
35 properties, thus, interferes with its function and leads to lipid bilayer stress (LBS)
36 (Covino et al., 2018). Maintaining the membranes' composition is therefore crucial for
37 a cell. High dietary intake of saturated fatty acids leads to a metabolic syndrome
38 referred to as lipotoxicity (Ertunc and Hotamisligil, 2016). On a cellular level, elevated
39 levels of saturated fatty acids alter membrane composition. Sensitive for these
40 changes is the endoplasmic reticulum, which is a major site for protein and lipid
41 synthesis, and the main intracellular calcium storage (Schwarz and Blower, 2016).
42 Lipid disequilibrium interferes with secretory capacity, and renders cells specialized in
43 secretion, such as insulin-producing beta cells, susceptible to cell death (Preston et
44 al., 2009, Acosta-Montaño and García-González 2018). Although LBS has been
45 suggested to play a major part in disease progression, the spectrum of the underlying
46 molecular players sensing LBS remains to be identified.

47 The unfolded protein (UPR) sensors IRE1, PERK1, and ATF6 have been found
48 to be sensitive for changes in membrane fluidity (Volmer et al., 2013; Koh et al., 2018).
49 On the molecular level, IRE1, PERK1, and ATF6 act in parallel in response to unfolded
50 proteins (Fig. 1a). Activated IRE1 splices *XBP1* mRNA to stabilize the transcript and
51 to allow translation of the spliced XBP1 transcription factor (Fig. 1a). PERK1
52 phosphorylates the initiation factor eIF2alpha, which reduces translation rate and
53 allows preferential translation of genes containing upstream open reading frames
54 (uORFs), such as the transcription factor ATF4 (Harding et al., 2000; Fig. 1a). During
55 ER stress, ATF6 translocates from the ER to the Golgi, where it is cleaved by proteases

56 called S1P and S2P. Cleaved ATF6 migrates to the nucleus and acts as a transcription
57 factor (Fig. 1a). The transcription factors co-regulate many targets, but how the
58 downstream targets of the three arms of the UPR restore membrane homeostasis in
59 detail remains unknown.

60 In *C. elegans*, loss of fatty acid desaturases *fat-6* and *fat-7* or the mediator *mdt-*
61 *15*, which regulates *fat-6/7* expression, leads to higher ratio of saturated fatty acids in
62 the membranes. This activates the ER stress reporter *hsp-4::gfp* via the IRE-1/XBP-1
63 axis (Hou et al., 2014). Activation of the ER stress sensor can also be achieved by
64 depleting the cell's phosphatidylcholine levels. Curiously, the signature of lipid bilayer
65 stress response is different from the canonical UPR in *C. elegans* (Hou et al., 2014;
66 Koh et al., 2018). This argues for an additional layer of regulation that fine-tunes the
67 output during activation of the three UPR arms (Fig. 1a).

68 Genetic mutant screening for members of the UPR have been successful
69 (Calfon et al., 2002; Singh and Aballay, 2017), but might have missed lethal genes.
70 RNAi-based forward screens can bypass genes that cause embryonal lethality or
71 developmental defects. However, feeding more than one RNAi simultaneously was
72 previously reported to produce poor results (Min et al., 2010). This suggests a
73 bottleneck for screening strategies where one would like to screen for suppressors of
74 a phenotype caused by a knock down using an RNAi-mediated screen.

75 The auxin inducible degradation (AID) has been introduced into *C. elegans*
76 recently (Zhang et al., 2015). A protein of interest can be tagged with a short 68 amino
77 acid sequence, which is recognized by the E3 ubiquitin ligase TIR1 derived from
78 *Arabidopsis thaliana* in the presence of a small molecule called auxin. Ubiquitination
79 targets the degron-tagged protein for fast degradation by the proteasome. Half times

80 less than 30 minutes have been reported for cytosolic proteins after transferring
81 animals co-expressing a degron-tagged protein and TIR1 on plates containing auxin
82 (Zhang et al., 2015). The AID is therefore faster and more efficient than RNAi. Since
83 AID initiates protein degradation and RNAi initiates mRNA degradation, these two
84 systems do not compete with each other and can be used in parallel.

85 Here, we identify suppressors of lipid bilayer stress using a novel approach by
86 combining AID and RNAi-based forward genetic screening. Knockdown of MDT-15 by
87 AID was used to induce LBS, which was visualized using the endoplasmic reticulum
88 stress sensors *Patf-4::gfp* and *Phsp-4::gfp*. We screened the RNAi libraries targeting
89 kinases and transcription factors for suppressors. Out of 868 genes, we identified 8
90 novel hits that robustly blocked LBS caused by MDT-15 knockdown.

91

92 **Material and Methods**

93 **Strains**

94 All strains were maintained at 20°C on OP50 *Escherichia coli* as described.

95 Strains used in this study are either available from CGC or upon request:

96 **IJ1729**: *ieSi57* [*Peft-3::TIR1::mRuby::unc-54* 3'UTR; *cb-unc-119*] II; *yh44* [*mdt-*
97 *15::degron::EmGFP*] III. (Lee et al., 2019)

98 **SJ4005**: *zcls4* [*Phsp-4::GFP*] V. (Harding et al., 2000)

99 **LD1499**: [*Patf-4(uORF)::GFP::unc-54(3'UTR)*]

100 **LSD2096**: *ieSi57* [*Peft-3::TIR1::mRuby::unc-54(3'UTR)*; *cb-unc-119*] II; *yh44* [*mdt-*
101 *15::degron::EmGFP*] III; [*Patf-4(uORF)::GFP::unc-54(3'UTR)*].

102 **LSD2102**: *ieSi57* [*Peft-3::TIR1::mRuby::unc-54* 3'UTR; *cb-unc-119*] II; *yh44* [*mdt-*
103 *15::degron::EmGFP*] III; *zcls4* [*Phsp-4::GFP*] V.

104 For generation of the screening strain, IJ1729 males was crossed with LD1499. 48 F2
105 were singled and their offspring were put on plates containing 100 µM Auxin and
106 checked for upregulation of the reporter (Fig. 2a). In parallel, IJ1729 was crossed to
107 SJ4005.

108

109 **Microscopy**

110 For image acquisition, the animals were put on freshly made 2% agar pads and
111 anesthetized with 1 mM tetramisole. Images were taken with an upright bright field
112 fluorescence microscope (Tritech Research, model: BX-51-F) and a camera of the
113 model DFK 23UX236 (Teuscher and Ewald, 2018).

114

115 **Preparation of Auxin**

116 70 mg of Auxin (3-Indoleacetic acid, Sigma #I3750) were dissolved in 10 ml DMSO to
117 yield a 40 mM stock solution and stored at 4°C. The stock was further diluted in M9
118 to 100 µM before use.

119

120 **Suppressor screen design**

121 A detailed step-by-step protocol can be found in the supplement and a schematic
122 outline is shown in Fig. 2b.

123 Briefly, 24-well plates were filled with NGM containing Ampicillin (100 µg/ml),
124 Tetracyclin (12.5 µg/ml) and 1mM IPTG, seeded with 50 µl of freshly grown RNAi
125 bacteria and dried in a sterile hood. On the next day, plates containing gravid LSD2096
126 adults were washed off and discarded and the laid eggs were scratched off and
127 collected. Approximately 30-40 eggs were pipetted into a well and incubated at 20°C.
128 After 48 hours, the wells were top coated with 50 µl of 100 µM Auxin, dried in a sterile
129 hood and put at 20°C overnight. The following day, the wells were screened for
130 suppression of the GFP signal. The kinase and transcription factor libraries were
131 screened twice. The preliminary hits had to successfully pass three additional runs on
132 6 cm plates.

133

134 **Heat-shock and tunicamycin treatment**

135 Animals, RNAi bacteria, and plates were prepared as above, without the addition of
136 auxin. Heat-shock was carried out for 1 hour at 37°C, incubated for 5 hours at 25°C,
137 and the animals were checked for GFP expression. Plates were top coated with 0.5 ml
138 of 35 µg/ml tunicamycin (Sigma, T7765), incubated for 6 hours at 25°C, and the
139 animals were checked for GFP expression.

140

141 Results and Discussion

142 To find a suitable reporter for screening, we used RNAi against *mdt-15* and *fat-6/7* and
143 found two reporters *Patf-4::gfp* and *Phsp-4::gfp* that are activated by LBS (Fig. 1b). For
144 screening, we preferred *Patf-4::gfp* over *Phsp-4::gfp* for its stronger induction of GFP.
145 Crossing *mdt-15(tm2182)* mutant with *Patf-4::gfp* led to a heterogeneous GFP
146 expression, making it impossible to use this strain for screening. We therefore switched
147 to an endogenously degron-tagged *mdt-15* strain (Lee et al., 2019). Unstressed MDT-
148 15::degron *C. elegans* expressed *Patf-4::gfp* only at basal levels at 20°C. Incubation
149 with 100 µM Auxin for 24 hours increased GFP levels drastically and homogenously
150 (Fig. 2a). We additionally observed typical *mdt-15* phenotypes such as small body size,
151 reduced brood size, and a pale appearance (Taubert et al., 2008; Lee et al., 2019).
152 Surprisingly, the eggs of untreated animals were sensitive to bleaching. Either, the
153 screening strain carries a background mutation or degron-tagged *mdt-15* is slightly
154 hypomorph. We continued with our screen by collecting laid eggs off the bacterial lawn.

155 To gain insights into LBS, we took a targeted RNAi approach. We decided to
156 screen through almost all *C. elegans* kinases (441 genes) and transcription factors
157 (427 genes; Fig. 2b). Our first-pass screening round resulted in 6 kinases and 31
158 transcription factors (Fig. 2b). To sort out false positives, we tested the preliminary hits
159 on 6 cm plates and ended up with 23 verified hits that block *Patf-4::gfp* induction (Fig.
160 2b, 2c; Supplementary Table 1). To test whether the hits are specific for lipid bilayer
161 stress, and not general inhibitors of the unfolded protein response, we heat-shocked
162 the animals and treated them with the N-glycosylation-inhibitor tunicamycin (Fig. 2b).
163 Most of the clones not passing this step were wrongly annotated GFP clones
164 (Supplementary Table 1). Reassuringly, we detected *xbp-1*, a transcription factor

165 spliced by IRE-1 (Supplementary Table 1). XPB-1 is known to upregulate *hsp-4* mRNA
166 during UPR (Calton et al., 2002). To rule out transgene-specific effects, we crossed
167 *Phsp-4::gfp* into *mdt-15::degron*;TIR1 and tested the hits that have passed the
168 previous steps (Fig. 2b). Only the weakest hit, *ztf-1*, did not pass this step
169 (Supplementary Table 1). We ended up with 9 high confidence hits, 8 of them not
170 previously described in *C. elegans* (Table 1). Taken together, with our novel approach
171 of combining AID and RNAi screening, we bypassed developmental and lethal
172 obstacles caused by depletion of *mdt-15*. Our screen revealed a known molecular
173 player (IRE-1), but also identified several new genes important to mount a proper LBS
174 response. Thus, our results provide a proof-of-concept and support the feasibility of
175 combined AID-RNAi screening approaches.

176

177 **Regulation of LBS by IRE-1 and XBP-1**

178 We unbiasedly detected IRE-1, which has previously been proposed as a sensor for
179 LBS in yeast and in *C. elegans*, and its target *xbp-1* (Thibault et al., 2012). This
180 confirms the selectivity of our screen. Unfolded proteins in the ER lead to IRE1
181 oligomerization and the subsequent stimulation of its endoribonuclease activity and
182 splicing of the transcription factor *xbp-1*. However, monomeric IRE1 still displays
183 RNase activity and splices XBP1 mRNA in HeLa cells during LBS (Kitai et al., 2013;
184 Ho et al., 2020). Spliced mRNA of *xbp-1* is much more stable than the unspliced
185 variant. IRE-1 is not needed for heat-shock or tunicamycin-induced UPR, but its target
186 *xbp-1* (Supplemental Table 1). We did not detect *pek-1* and *atf-6*, the other members
187 of the canonical UPR. Thus, we confirmed that IRE-1 branch acts as a major sensor
188 of LBS.

189

190 ***Immunity response network regulates lipid bilayer stress***

191 Knocking down phosphatidylcholine synthesis leads to activation of genes involved in
192 the immune response (Koh et al., 2018). Many of these transcripts are upregulated in
193 an IRE-1-dependent manner. In addition to *ire-1*, we detected the NRF1,2,3
194 homologue *skn-1* and the GATA transcription factor *elt-2*. Both are involved in p38-
195 mediated innate immunity (Block et al., 2015; Blackwell et al., 2015). RNAi of *skn-1*
196 was one of our strongest suppressors (Fig. 1c). SKN-1 is a major transcription factor
197 for promoting oxidative stress resistance (Blackwell et al., 2015). There are four
198 isoforms of SKN-1: *skn-1a*, *b*, *c*, *d* (Blackwell et al., 2015). A previous study
199 demonstrated that IRE-1 has an additional mode of action in its monomeric state:
200 elevated levels of reactive oxygen species leads to sulfenylation of cysteine residues
201 in IRE-1 and activates SKN-1a via the p38 MAPK (Glover-Cutter et al., 2013; Hourihan
202 et al., 2016). Isoform *skn-1a* is similar to mammalian NRF1, which regulates
203 proteostasis and is a transmembrane protein located in the ER (Lehrbach and Ruvkun,
204 2016; Wang and Chan, 2006). Curiously, *mdt-15* and *skn-1c*, but not *skn-1a*, co-
205 regulate targets involved in detoxification such as *gst-4* (Goh et al., 2014). This
206 suggests that SKN-1a is not only activated by loss of *mdt-15*, but also works
207 independently of MDT-15. *skn-1* knockdown does not only block LBS response, but
208 also reverses the small body size and the small amount of eggs laid (although these
209 eggs do not hatch because *skn-1* knockdown is embryonic lethal). This suggests that
210 some of the observed phenotypes in *mdt-15* mutants or knockdowns are *skn-1*-
211 dependent. The mammalian SKN-1c orthologue NRF2 has been shown to have
212 protective functions during palmitate-induced lipotoxicity in mammalian cells (Cunha et

213 al., 2016; Park et al., 2015). Taken together, this suggests a potential isoform-specific
214 role for SKN-1a during LBS.

215 *elt-2* is a GATA transcription factor that is essential for the mesodermal cell fate
216 and development of the intestine. While null mutants of *elt-2* are embryonic lethal, post-
217 developmental knockdown shortens lifespan and overexpression extends lifespan
218 (Mann et al., 2016). We observed developmental arrest after *elt-2* knockdown. These
219 arrested larvae were still susceptible to heat and tunicamycin treatments, indicating
220 that the UPR was still intact. Similar to *skn-1*, *elt-2* is recruited to promoters during
221 *Pseudomonas aeruginosa* infection and co-regulates targets in a p38-mediated
222 fashion (Block et al., 2015). Furthermore, *elt-2* and *mdt-15* cooperate during heavy
223 metal intoxication (Shomer et al., 2019), strengthening the existence of a transcription
224 factor network that cooperatively regulates different stress responses.

225

226 ***Modulators and activators of the LBS response (let-607, gsk-3 and drl-1)***

227 We found three genes, *let-607*, *gsk-3*, and *drl-1*, implicated in modulating the ER stress
228 responses. RNAi of *let-607* suppressed the activation of the *atf-4* reporter completely
229 (Fig. 2c). *let-607* is, together with *crh-1* and *crh-2*, one of the CREB3 orthologues in *C.*
230 *elegans*. The mammalian Creb3 family consists of five members (CREB3/Luman,
231 CREB3L1/OASIS, CREB3L2/BBF2H7, CREB3L3/CREBH, and CREB3L4) and is
232 related to ATF6 and SREBP (Sampieri et al., 2019). All of them are localized in the ER
233 and are similar to ATF6 activated by anterograde transport to the Golgi and subsequent
234 cleavage by S1P or S2P. In humans and mice, CREB3L2 upregulates SEC23 and
235 controls secretory load, especially during bone formation (Saito et al., 2009; Tomoishi
236 et al., 2017; Al-Maskari et al., 2018; Khetchoumian et al., 2019). CREB3 and CREB3L3

237 are induced after palmitate-induced ER stress and knock down of CREB3 by siRNA
238 sensitizes human islet cells to palmitate-induced ER stress (Cnop et al., 2014). CREB3
239 has been identified in regulating Golgi-stress and activates ARF4 (Reiling et al., 2013).
240 A previous study in *C. elegans* links *let-607* with the upregulation of *sec-23* and other
241 proteins involved in secretion (Weicksel et al., 2016). *let-607* has also been identified
242 in a screen for suppressors of PolyQ aggregation and suppresses motility defects
243 caused by mutations in the paramyosin ortholog UNC-15, the basement-membrane
244 protein perlecan UNC-52, the myosin-assembly protein UNC-45, and the myosin
245 heavy chain UNC-54 (Silva et al., 2011). In addition, knock down of *let-607* increased
246 expression of cytosolic heat-shock proteins. Based on these previous observations
247 and our results, we propose that *let-607*/CREB3 family is sensing LBS and acts
248 together with the other identified transcription factor encoding genes *xbp-1*, *skn-1*, and
249 *elt-2* to mount a unique stress response that is different from the canonical UPR.

250 *drl-1*, also known as *mekk-3*, has been found in a screen looking for enhancers
251 of dauer formation and extends lifespan by simulating dietary restricted-like conditions
252 (Chamoli et al., 2014). Curiously, loss of *drl-1* causes a pale appearance of the animals
253 resembling *fat-6/7* and *mdt-15* mutants, but the mode-of-action seems to be different.
254 The *drl-1* promoter is expressed in vulval muscles, body wall muscles, hypodermis,
255 seam cells, some neurons, and tissues lining the pharynx and anus, but not the
256 intestine. Additionally, knockdown in the intestine using tissue-specific RNAi did not
257 extend lifespan (Chamoli et al., 2014). Knockdown of MDT-15 activates *Patf-4::gfp* and
258 *Phsp-4::gfp* expression mainly in the intestine (Fig 1b). Therefore, knockdown of *drl-1*
259 acts in a cell non-autonomous manner. *drl-1* decreases fat storage by upregulating
260 fatty acid oxidation (Chamoli et al., 2014). The *C. elegans* orthologue of the
261 ribonuclease Regnase-1, *rege-1*, shares many upregulated genes and causes a pale

262 appearance without activation of LBS (Supplementary Table 1; Habacher et al. 2016).
263 This suggests a link between *drl-1* and *rege-1*. However, knockdown of *rege-1* does
264 not phenocopy loss of *drl-1* (Supplementary Table 1). Despite the striking similarities
265 shared by *rege-1* and *drl-1*, only *drl-1* modulates LBS. Intriguingly, *drl-1* knockdown
266 itself causes ER stress at the L2 stage and this mounts a protective effect throughout
267 life (Matai et al., 2019). Since *drl-1* rewires metabolism by mimicking dietary restriction,
268 we speculate that activation of fatty acid oxidation protects from lipotoxicity. Indeed,
269 we observed that starved animals in wells with no food did not upregulate the reporter.

270 The glycogen synthase kinase-3 (*gsk-3*) has been described as the busiest of
271 all kinases with over 100 targets known, and was found to attenuate palmitate-induced
272 apoptosis (Beurel et al., 2015; Ibrahim et al., 2011). Paradoxically, *gsk-3* inhibits *skn-*
273 *1* and stabilizes CREB3, both contradicting with the results of our screen (An et al.,
274 2005; Barbosa et al., 2013). If it does not act on the other hits, what could be its mode
275 of action? Activation of the lipid bilayer stress activates autophagy via the IRE-1/XBP-
276 1 axis (Ho et al., 2020). Blocking autophagy in this context causes sickness, sterility
277 and developmental defects. Intriguingly, GSK3 inhibition activates autophagy (Parr et
278 al., 2012). We therefore speculate that prior knock down of GSK3 leads to an elevated
279 rate of autophagy, which protects from LBS and ameliorates the stress response.

280

281 **General players in gene expression, but specific for LBS**

282 The last three hits consist of *gtf-2f2*, *ntl-4*, and *rpl-14*, which are involved in
283 transcription, RNA processing, and translation, respectively. Interestingly, although
284 with RNAi against *gtf-2f2*, *ntl-4*, and *rpl-14* inactivate general processes, the heat- or

285 tunicamycin induced UPR is still functioning and is not affected. This favors the model
286 that UPR and LBS are differentially regulated (Fig. 3).

287

288 **Summary**

289 We report the identification of 8 novel regulators of the lipid bilayer stress response.

290 We grouped them into three categories (Fig. 3). *skn-1* and *elt-2*, together with the
291 previously characterized *ire-1*, are transcription factors involved in immune response.

292 *let-607* might be activated in parallel with the canonical UPR arms, and *drl-1* and *gsk-*
293 *3* modulate the ER stress response in our suggested model upstream or downstream,

294 respectively. The last category consists of genes involved in general processes of gene

295 expression. Furthermore, we highlight the potential of combining AID and RNAi-based
296 genetic screens.

297

298 **Acknowledgement**

299 We thank Chi Yun and David Ron for the *Patf-4::gfp* strain, Seung-Jae V. Lee for the

300 *mdt-15::degron* strain, Gary Ruvkun for kinase and transcription factor RNAi libraries,

301 Keith Blackwell and Ewald Lab members for comments on the manuscript. Some

302 strains were provided by the CGC, which is funded by NIH Office of Research

303 Infrastructure Programs (P40 OD010440). Funding from the Swiss National Science

304 Foundation PP00P3_163898 to CYE and ETH Research Foundation Grant ETH-30

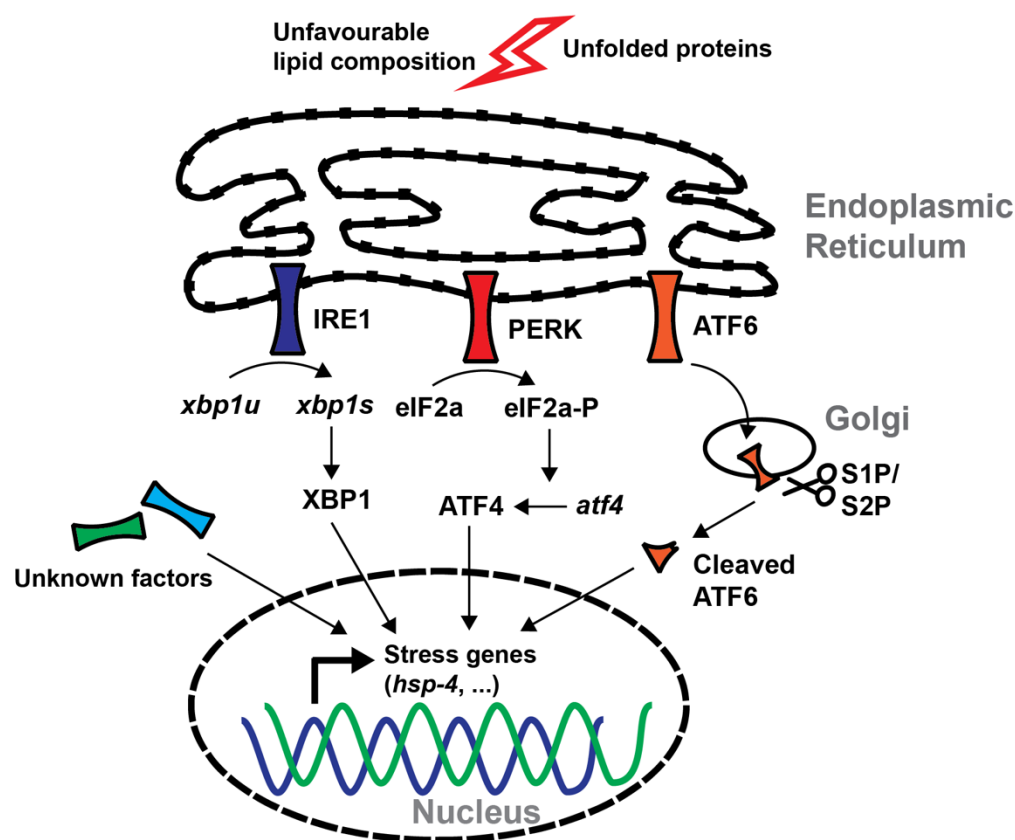
305 16-2 to RV.

306

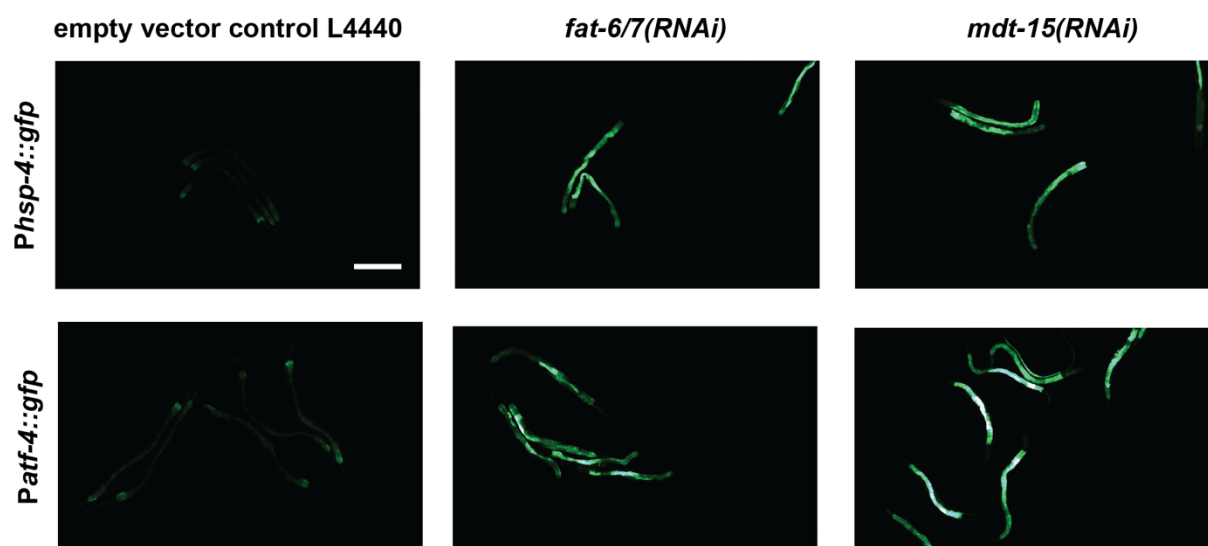
307

308 **Figures**

a



b



309

310 **Figure 1. Integrated stress response of *C. elegans***

311 a) Model of the unfolded protein and lipid bilayer stress response.

312 b) *Phsp-4::gfp* and *Patf-4::gfp* are activated by *fat-6/7(RNAi)* and *mdt-15(RNAi)*.

313 Bar = 200 μ m.

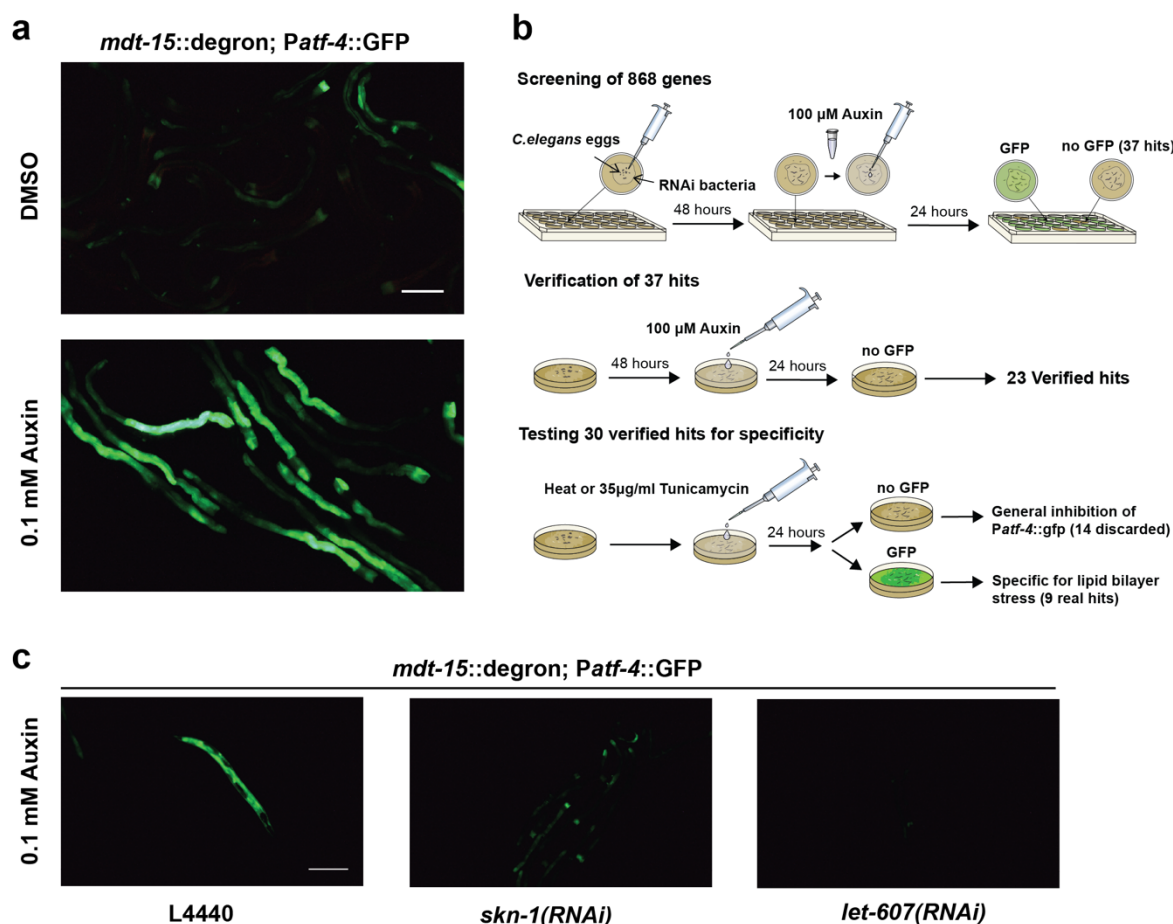


Table 1

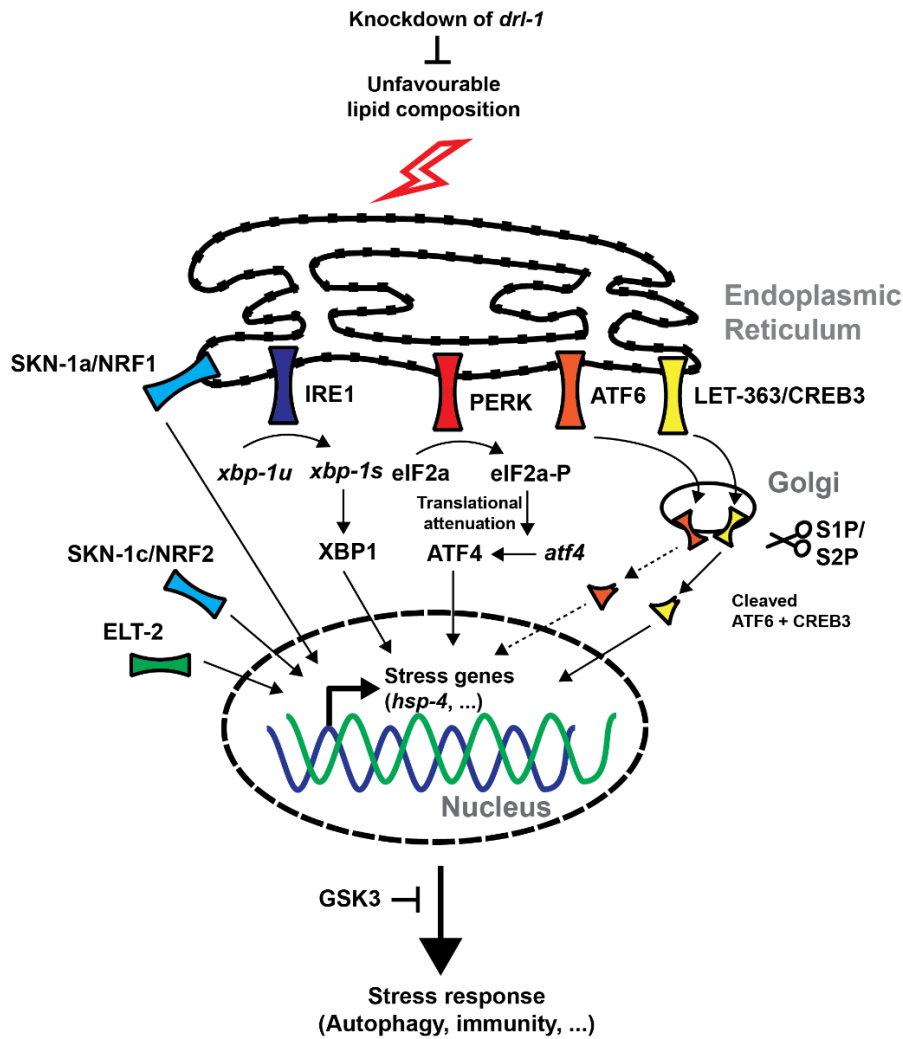
Gene name	Level of repression	Short description
<i>drl-1</i>	Full	Orthologue of mitogen-activated protein kinase kinase kinase 3 isoforms
<i>rpl-14</i>	Full	Protein of the large ribosomal subunit (60S)
<i>let-607</i>	Full	Orthologue of the CAMP Responsive Element Binding Protein 3 (CREB3) transcription factor family
<i>gsk-3</i>	Strong	Orthologue of human GSK3B (glycogen synthase kinase 3 beta)
<i>ire-1</i>	Strong	Inositol-requiring Enzyme 1, a sensor of the UPR
<i>ntl-4</i>	Strong	Orthologue of human CCR4-NOT Transcription Complex Subunit 4 (CNOT4)
<i>gtf-2F2</i>	Strong	Orthologue of human (general transcription factor IIF subunit 2 (GTF2F2)
<i>elt-2</i>	Strong	Orthologue of the transcription factors GATA4/6
<i>skn-1</i>	Strong	Orthologue of the transcription factor Nuclear factor erythroid 2-related factor 2 (NRF2)

314

315 **Figure 2. Suppressor screen of LBS**

- 316 a) Addition of 0.1 mM Auxin degrades *mdt-15::degron* and leads to expression of
 317 *Patf-4::gfp* in LSD2096. Pictures were taken 24 h after Auxin addition. Bar = 200
 318 μm
 319 b) Summary of the screening outline.
 320 c) Addition of 0.1 mM Auxin to degrade *mdt-15::degron* after *skn-1* and *let-607*
 321 RNAi represses activation of *Patf-4::gfp* in LSD2096. Pictures were taken 24 h
 322 after Auxin addition. Bar = 200 μm

323



324

325 **Figure 3. Hypothetical model of LBS in *C. elegans***

326 Updated model of LBS in *C. elegans* indicates a complex network of transcription
327 factors and up- and downstream modulators. 6 out of 9 our hits are included in this
328 model.

329

330 **Supplemental files are available at FigShare.**

331 Supplementary File1 contains the protocol for 24-well plates AID-RNAi screen.

332 Supplementary Table1 contains the lipotoxicity AID-RNAi screen results.

333

334 **References**

335 Acosta-Montaño, P., & García-González, V. (2018). Effects of dietary fatty
336 acids in pancreatic beta cell metabolism, implications in homeostasis. *Nutrients*,
337 *10*(4), 393.

338
339 Al-Maskari, M., Care, M. A., Robinson, E., Cocco, M., Tooze, R. M., & Doody,
340 G. M. (2018). Site-1 protease function is essential for the generation of antibody
341 secreting cells and reprogramming for secretory activity. *Scientific reports*, *8*(1), 1-11.

342
343 An, J. H., Vranas, K., Lucke, M., Inoue, H., Hisamoto, N., Matsumoto, K., &
344 Blackwell, T. K. (2005). Regulation of the *Caenorhabditis elegans* oxidative stress
345 defense protein SKN-1 by glycogen synthase kinase-3. *Proceedings of the National*
346 *Academy of Sciences*, *102*(45), 16275-16280.

347
348 Barbosa, S., Fasanella, G., Carreira, S., Llarena, M., Fox, R., Barreca, C., ... &
349 O'Hare, P. (2013). An Orchestrated Program Regulating Secretory Pathway Genes
350 and Cargos by the Transmembrane Transcription Factor CREB-H. *Traffic*, *14*(4),
351 382-398.

352
353 Beurel, E., Grieco, S. F., & Jope, R. S. (2015). Glycogen synthase kinase-3
354 (GSK3): regulation, actions, and diseases. *Pharmacology & therapeutics*, *148*, 114-
355 131.

356
357 Blackwell, T. K., Steinbaugh, M. J., Hourihan, J. M., Ewald, C. Y., & Isik, M.
358 (2015). SKN-1/Nrf, stress responses, and aging in *Caenorhabditis elegans*. *Free*
359 *Radical Biology and Medicine*, *88*, 290-301.

360
361 Block, D. H., Twumasi-Boateng, K., Kang, H. S., Carlisle, J. A., Hanganu, A.,
362 Lai, T. Y. J., & Shapira, M. (2015). The developmental intestinal regulator ELT-2
363 controls p38-dependent immune responses in adult *C. elegans*. *PLoS genetics*,
364 *11*(5).

365

366 Chamoli, M., Singh, A., Malik, Y., & Mukhopadhyay, A. (2014). A novel kinase
367 regulates dietary restriction-mediated longevity in *Caenorhabditis elegans*. *Aging*
368 *Cell*, 13(4), 641-655.

369
370 Cnop, M., Abdulkarim, B., Bottu, G., Cunha, D. A., Igoillo-Esteve, M., Masini,
371 M., ... & Bugliani, M. (2014). RNA sequencing identifies dysregulation of the human
372 pancreatic islet transcriptome by the saturated fatty acid palmitate. *Diabetes*, 63(6),
373 1978-1993.

374
375 Covino, R., Hummer, G., & Ernst, R. (2018). Integrated functions of membrane
376 property sensors and a hidden side of the unfolded protein response. *Molecular cell*,
377 71(3), 458-467.

378
379 Cunha, D. A., Cito, M., Carlsson, P. O., Vanderwinden, J. M., Molkentin, J. D.,
380 Bugliani, M., ... & Cnop, M. (2016). Thrombospondin 1 protects pancreatic β -cells
381 from lipotoxicity via the PERK–NRF2 pathway. *Cell Death & Differentiation*, 23(12),
382 1995-2006.

383
384 Calfon, M., Zeng, H., Urano, F., Till, J. H., Hubbard, S. R., Harding, H. P., ... &
385 Ron, D. (2002). IRE1 couples endoplasmic reticulum load to secretory capacity by
386 processing the XBP-1 mRNA. *Nature*, 415(6867), 92-96.

387
388 Ertunc, M. E., & Hotamisligil, G. S. (2016). Lipid signaling and lipotoxicity in
389 metaflammation: indications for metabolic disease pathogenesis and treatment.
390 *Journal of lipid research*, 57(12), 2099-2114.

391
392 Glover-Cutter, K. M., Lin, S., & Blackwell, T. K. (2013). Integration of the
393 unfolded protein and oxidative stress responses through SKN-1/Nrf. *PLoS genetics*,
394 9(9).

395
396 Goh, G. Y., Martelli, K. L., Parhar, K. S., Kwong, A. W., Wong, M. A., Mah, A.,
397 ... & Taubert, S. (2014). The conserved Mediator subunit MDT-15 is required for
398 oxidative stress responses in *Caenorhabditis elegans*. *Aging Cell*, 13(1), 70-79.

399

400 Habacher, C., Guo, Y., Venz, R., Kumari, P., Neagu, A., Gaidatzis, D., ... &
401 Ciosk, R. (2016). Ribonuclease-mediated control of body fat. *Developmental cell*,
402 *39*(3), 359-369.

403

404 Harding, H. P., Novoa, I., Zhang, Y., Zeng, H., Wek, R., Schapira, M., & Ron,
405 D. (2000). Regulated translation initiation controls stress-induced gene expression in
406 mammalian cells. *Molecular cell*, *6*(5), 1099-1108.

407

408 Ho, N., Wu, H., Xu, J., Koh, J. H., Yap, W. S., Goh, W. W. B., ... & Thibault, G.
409 (2020). Stress sensor Ire1 deploys a divergent transcriptional program in response to
410 lipid bilayer stress. *Journal of Cell Biology*, *219* (7): e201909165.

411

412 Hou, N. S., Gutschmidt, A., Choi, D. Y., Pather, K., Shi, X., Watts, J. L., ... &
413 Taubert, S. (2014). Activation of the endoplasmic reticulum unfolded protein
414 response by lipid disequilibrium without disturbed proteostasis in vivo. *Proceedings of*
415 *the National Academy of Sciences*, *111*(22), E2271-E2280.

416

417 Hourihan, J. M., Mazzeo, L. E. M., Fernández-Cárdenas, L. P., & Blackwell, T.
418 K. (2016). Cysteine sulfenylation directs IRE-1 to activate the SKN-1/Nrf2 antioxidant
419 response. *Molecular cell*, *63*(4), 553-566.

420

421 Ibrahim, S. H., Akazawa, Y., Cazanave, S. C., Bronk, S. F., Elmi, N. A., Werneburg,
422 N. W., ... & Gores, G. J. (2011). Glycogen synthase kinase-3 (GSK-3) inhibition
423 attenuates hepatocyte lipoapoptosis. *Journal of hepatology*, *54*(4), 765-772.

424

425 Koh, J. H., Wang, L., Beaudoin-Chabot, C., & Thibault, G. (2018). Lipid bilayer
426 stress-activated IRE-1 modulates autophagy during endoplasmic reticulum stress. *J*
427 *Cell Sci*, *131*(22), jcs217992.

428

429 Khetchoumian, K., Balsalobre, A., Mayran, A., Christian, H., Chénard, V., St-
430 Pierre, J., & Drouin, J. (2019). Pituitary cell translation and secretory capacities are

431 enhanced cell autonomously by the transcription factor Creb3l2. *Nature*
432 *communications*, 10(1), 1-13.

433

434 Kitai, Y., Ariyama, H., Kono, N., Oikawa, D., Iwawaki, T., & Arai, H. (2013).
435 Membrane lipid saturation activates IRE 1 α without inducing clustering. *Genes to*
436 *Cells*, 18(9), 798-809.

437

438 Lee, D., An, S. W. A., Jung, Y., Yamaoka, Y., Ryu, Y., Goh, G. Y. S., ... & Lee,
439 S.V (2019). MDT-15/MED15 permits longevity at low temperature via enhancing
440 lipidostasis and proteostasis. *PLoS biology*, 17(8).

441

442 Lehrbach, N. J., & Ruvkun, G. (2019). Endoplasmic reticulum-associated
443 SKN-1A/Nrf1 mediates a cytoplasmic unfolded protein response and promotes
444 longevity. *Elife*, 8, e44425.

445

446 Mann, F. G., Van Nostrand, E. L., Friedland, A. E., Liu, X., & Kim, S. K. (2016).
447 Deactivation of the GATA transcription factor ELT-2 is a major driver of normal aging
448 in *C. elegans*. *PLoS genetics*, 12(4).

449

450 Matai, L., Sarkar, G. C., Chamoli, M., Malik, Y., Kumar, S. S., Rautela, U., ... &
451 Mukhopadhyay, A. (2019). Dietary restriction improves proteostasis and increases
452 life span through endoplasmic reticulum hormesis. *Proceedings of the National*
453 *Academy of Sciences*, 116(35), 17383-17392.

454

455 Min, K., Kang, J., & Lee, J. (2010). A modified feeding RNAi method for simultaneous
456 knock-down of more than one gene in *Caenorhabditis elegans*. *Biotechniques*, 48(3),
457 229-232.

458

459 Park, J. S., Kang, D. H., & Bae, S. H. (2015). Concerted action of p62 and
460 Nrf2 protects cells from palmitic acid-induced lipotoxicity. *Biochemical and*
461 *biophysical research communications*, 466(1), 131-137.

462

463 Parr, C., Carzaniga, R., Gentleman, S. M., Van Leuven, F., Walter, J., &
464 Sastre, M. (2012). Glycogen synthase kinase 3 inhibition promotes lysosomal
465 biogenesis and autophagic degradation of the amyloid- β precursor protein. *Molecular*
466 *and cellular biology*, 32(21), 4410-4418.

467
468 Preston, A. M., Gurisik, E., Bartley, C., Laybutt, D. R., & Biden, T. J. (2009).
469 Reduced endoplasmic reticulum (ER)-to-Golgi protein trafficking contributes to ER
470 stress in lipotoxic mouse beta cells by promoting protein overload. *Diabetologia*,
471 52(11), 2369-2373.

472
473 Reiling, J. H., Olive, A. J., Sanyal, S., Carette, J. E., Brummelkamp, T. R.,
474 Ploegh, H. L., ... & Sabatini, D. M. (2013). A CREB3-ARF4 signalling pathway
475 mediates the response to Golgi stress and susceptibility to pathogens. *Nature cell*
476 *biology*, 15(12), 1473-1485.

477
478 Saito, A., Hino, S. I., Murakami, T., Kanemoto, S., Kondo, S., Saitoh, M., ... &
479 Ikawa, M. (2009). Regulation of endoplasmic reticulum stress response by a
480 BBF2H7-mediated Sec23a pathway is essential for chondrogenesis. *Nature cell*
481 *biology*, 11(10), 1197-1204.

482
483 Sampieri, L., Di Giusto, P., & Alvarez, C. (2019). CREB3 transcription factors:
484 ER-Golgi stress transducers as hubs for cellular homeostasis. *Frontiers in Cell and*
485 *Developmental Biology*, 7, 123.

486
487 Schwarz, D. S., & Blower, M. D. (2016). The endoplasmic reticulum: structure,
488 function and response to cellular signaling. *Cellular and Molecular Life Sciences*,
489 73(1), 79-94.

490
491 Shomer, N., Kadhim, A. Z., Grants, J. M., Cheng, X., Alhusari, D., Bhanshali, F., ... &
492 Shih, J. (2019). Mediator subunit MDT-15/MED15 and Nuclear Receptor HIZR-
493 1/HNF4 cooperate to regulate toxic metal stress responses in *Caenorhabditis*
494 *elegans*. *PLoS Genetics*, 15(12).

495

496 Silva, M. C., Fox, S., Beam, M., Thakkar, H., Amaral, M. D., & Morimoto, R. I.
497 (2011). A genetic screening strategy identifies novel regulators of the proteostasis
498 network. *PLoS genetics*, 7(12).

499
500 Singh, J., & Aballay, A. (2017). Endoplasmic reticulum stress caused by
501 lipoprotein accumulation suppresses immunity against bacterial pathogens and
502 contributes to immunosenescence. *MBio*, 8(3), e00778-17.

503
504 Taubert, S., Hansen, M., Van Gilst, M. R., Cooper, S. B., & Yamamoto, K. R.
505 (2008). The Mediator subunit MDT-15 confers metabolic adaptation to ingested
506 material. *PLoS genetics*, 4(2).

507
508 Teuscher, A. C. & Ewald, C. Y. Overcoming Autofluorescence to Assess GFP
509 Expression During Normal Physiology and Aging in *Caenorhabditis elegans*. *BIO-*
510 *PROTOCOL* 8, (2018).

511
512 Thibault, G., Shui, G., Kim, W., McAlister, G. C., Ismail, N., Gygi, S. P., ... &
513 Ng, D. T. (2012). The membrane stress response buffers lethal effects of lipid
514 disequilibrium by reprogramming the protein homeostasis network. *Molecular cell*,
515 48(1), 16-27.

516
517 Tomoishi, S., Fukushima, S., Shinohara, K., Katada, T., & Saito, K. (2017).
518 CREB3L2-mediated expression of Sec23A/Sec24D is involved in hepatic stellate cell
519 activation through ER-Golgi transport. *Scientific reports*, 7(1), 1-11.

520
521 Volmer, R., van der Ploeg, K., & Ron, D. (2013). Membrane lipid saturation
522 activates endoplasmic reticulum unfolded protein response transducers through their
523 transmembrane domains. *Proceedings of the National Academy of Sciences*,
524 110(12), 4628-4633.

525
526 Wang, W., & Chan, J. Y. (2006). Nrf1 is targeted to the endoplasmic reticulum
527 membrane by an N-terminal transmembrane domain Inhibition of nuclear

528 translocation and transacting function. *Journal of Biological Chemistry*, 281(28),
529 19676-19687.

530

531 Weicksel, S. E., Mahadav, A., Moyle, M., Cipriani, P. G., Kudron, M., Pincus,
532 Z., ... & Fernandez, A. G. (2016). A novel small molecule that disrupts a key event
533 during the oocyte-to-embryo transition in *C. elegans*. *Development*, 143(19), 3540-
534 3548.

535

536 Zhang, L., Ward, J. D., Cheng, Z., & Dernburg, A. F. (2015). The auxin-
537 inducible degradation (AID) system enables versatile conditional protein depletion in
538 *C. elegans*. *Development*, 142(24), 4374-4384.

539

540

541